Supplemental Material

Journal of Climate

Changes of Decadal SST Variations in the Subpolar North Atlantic under Strong CO_2 Forcing as an Indicator for the Ocean Circulation's Contribution to Atlantic Multidecadal Variability

https://doi.org/10.1175/JCLI-D-18-0739.1

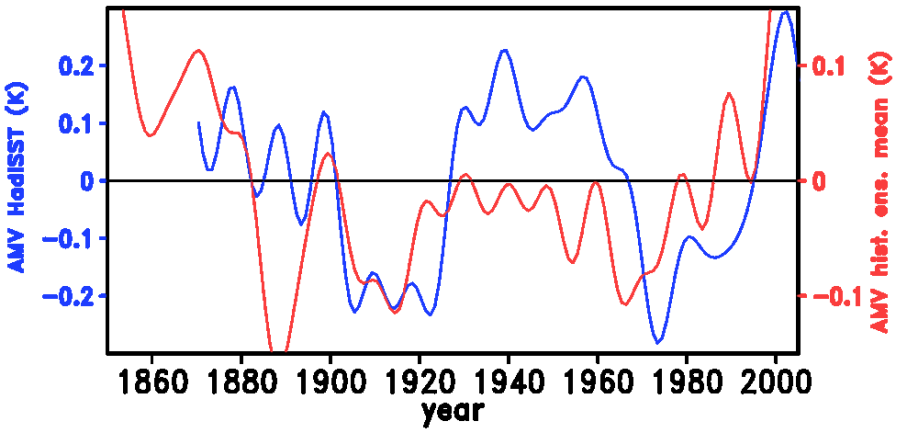

Figure S.1: AMV time series for observations (HadISST, blue) and the ensemble mean of the historical ensemble (solid red). To allow a better comparison of the shape of the graphs, both timeseries have different scaling as indicated by the axis to the left/right of the plot. Both timeseries were detrended by removing a linear fit to the ensemble mean of the historical ensemble. Data are 10-year low-pass-filtered.

(a) 10year lowpass-filtered

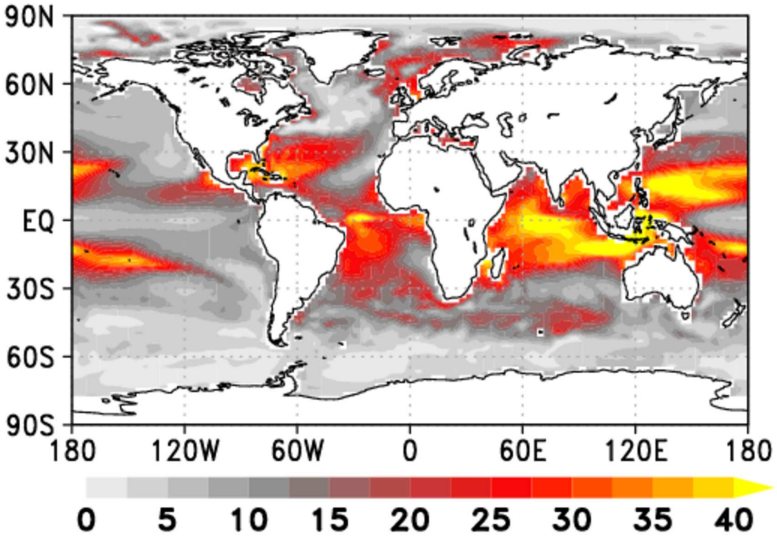

(b) 20year lowpass-filtered

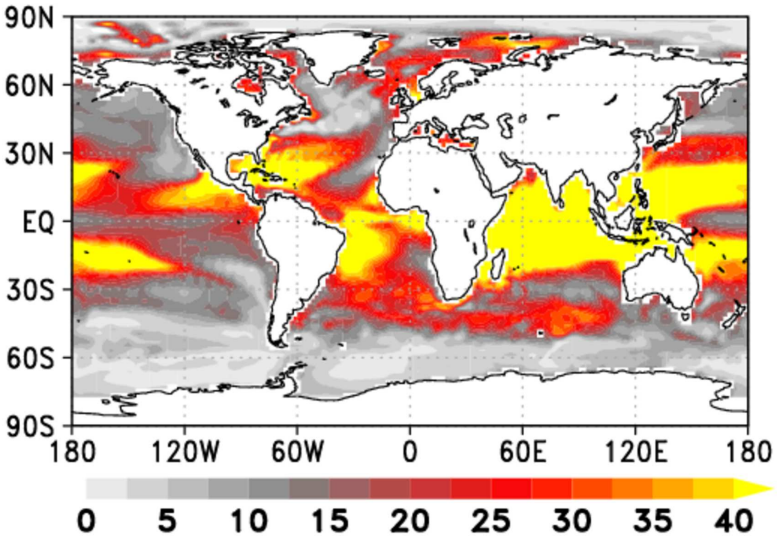

Figure S.2: SST Variance (in %) explained by the external forcing as the fraction between the variance of the ensemble mean divided by the averaged variances of the individual ensemble members. In (a) SSTs were 10-year-lowpass-filtered, in (b) SSTs were 20-year-lowpass-filtered (as in Bellomo et al. 2018). In both cases SSTs were detrended by removing a linear fit to the ensemble mean.

(a) AMV pictl (lin. trend removed)

(b) AMV hist (ensmean trend removed)

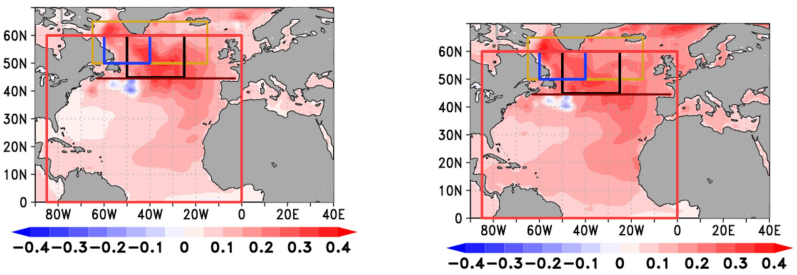

Figure S.3: Spatial structure of the AMV in the (a) pre-industrial control simulation and (b) the historical ensemble. Regression of the SST on the normalized field average (85°W to 0°W, 0°to 60°N) of SST (in K/standard deviation) in HadISST. Before hand SSTs were detrended by removing a linear fit (for pictl)/a linear fit to the ensemble mean (for the historical ensemble) and a 10-year lowpass-filter was applied. Boxes indicate the regions for the definition of the indices (for details refer to the caption of Fig.1 in the main paper.).

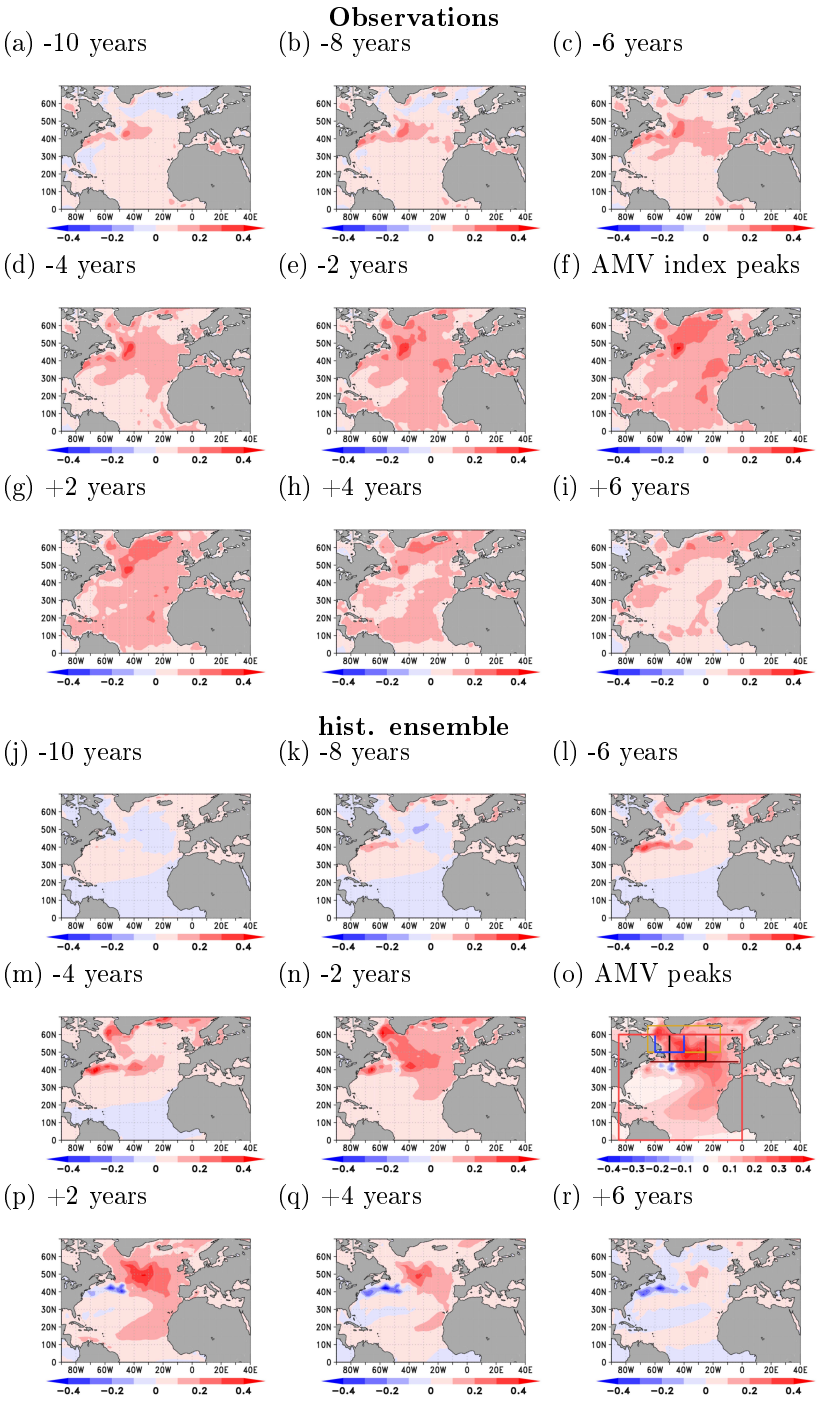

Figure S.4: evolution of the AMV (defined as in section 2c) for different lags for observations (a-i) and the historical ensemble (j-r)

.

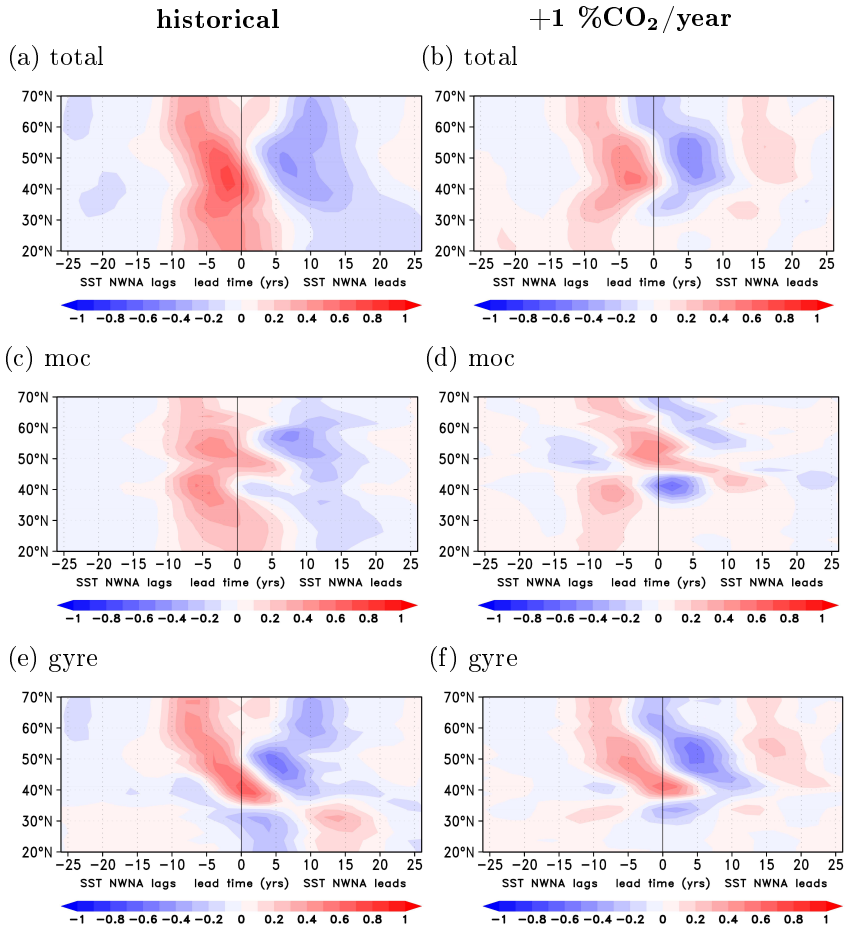

Figure S.5: Correlation of the convergence of northward ocean heat transport in the Atlantic on the SST box mean in the northwest North Atlantic in the historical ensemble (left) and the ensemble with an incremental SST increase by $+1\%CO_2$/year (right) for the total ocean heat transport ((a) & (b)) and separated for the overturning ((c) & (d)) and the gyre heat transport ((e) & (f)). All data were 10 year lowpass-filtered and the trend/external signal was removed by subtracting the ensemble means.

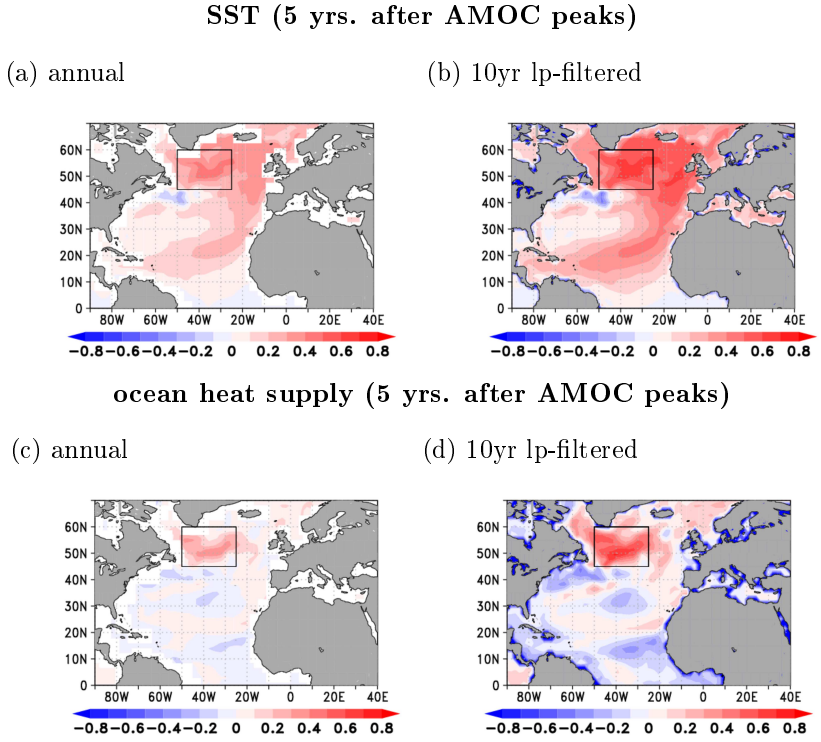

Figure S.6: Correlation between the AMOC at 45°N and SST (top) and the ocean heat supply (computed for each grid cell individually, bottom) at a lag of 5 years in the historical simulations. The black box indicates the region that we refer to as "the north-western North Atlantic". For the left column the correlations were computed on annual mean values, for the right column a 10-year lowpass filter was applied before. All data were detrended by removing the ensemble mean of the according quantity.

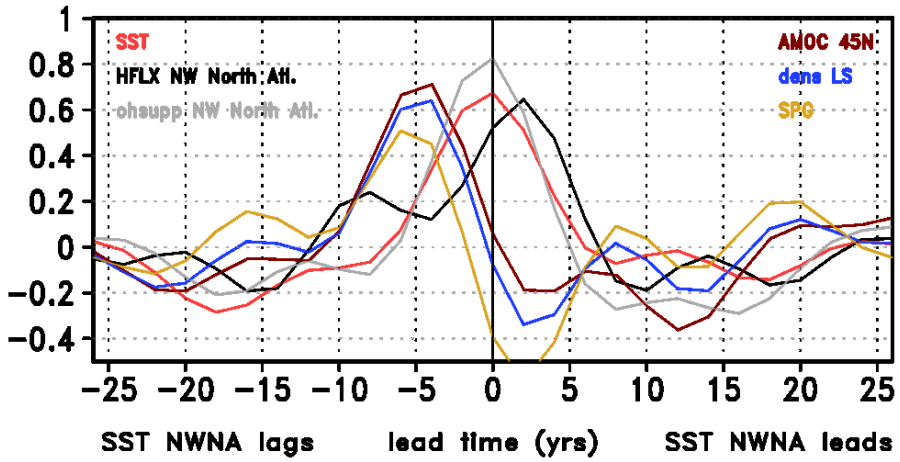

Figure S.7: Lag-correlations of the SST box mean in a box in the north-west Atlantic (region 50-25°W, 45-60N°, i.e. the black box in Fig. S.3b) with different indices of decadal climate variability in the pre-industrial control run. Colours indicate lag-crosscorrelations with the AMV index (red, defined as in section 2c, averaged for the red box in Fig. S.3b), with the ocean-atmosphere turbulent heat flux in the same box (black, positive upwards), the ocean heat supply as the residual between the ocean heat content change integrated over the box minus the turbulent flux to the atmosphere (grey), the AMOC (as the overturning stream function at 1000m depth) at 45°N (brown), the Labrador Sea mixed layer depth (blue, the box average for a box 70-40°W, 50-70°N, i.e. the blue box in Fig. S.3b), and the Subpolar Gyre strength (orange) as the field minimum of the barotropic stream function in the region 65-15°W, 50-65°N (i.e. the green box in Fig. S.3b) multiplied by -1 to get positive values for a stronger SPG. All time-series were 10-year-lowpass-filtered and linearly detrended.

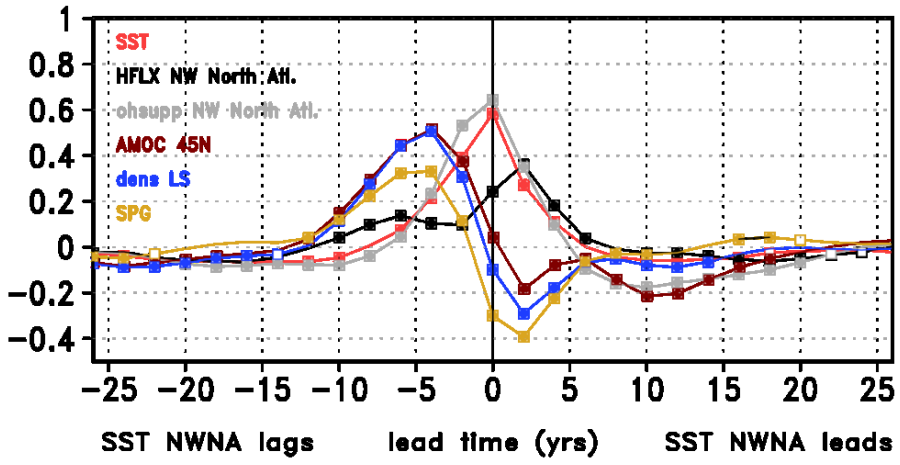

Figure S.8: Lag-correlations of the SST box mean in a box in the north-west Atlantic (region 50-25°W, 45-60°, i.e. the black box in Fig. S.3b) with different indices of decadal climate variability in the historical ensemble for annual data (i.e. without applying a decadal lowpass filter). Colours indicate lag-crosscorrelations with the AMV index (red, defined as in Fig. S.3b), with the ocean-atmosphere turbulent heat flux in the same box (black, positive upwards), the ocean heat supply as the residual between the ocean heat content change integrated over the box minus the turbulent flux to the atmosphere (grey), the AMOC (as the overturning stream function at 1000m depth) at 45°N (brown), the Labrador Sea 3-dimensionally averaged deep ocean density (blue, the box average for a box 60-40°W, 50-60°N, i.e. the blue box in Fig. S.3b between 1500 m and 3000 m water depth), and the Subpolar Gyre strength (orange) as the field minimum of the barotropic stream function in the region 65-15°W, 50-65°N (i.e. the green box in Fig. S.3b) multiplied by -1 to get positive values for a stronger SPG. Non-filled (filled) markers indicate significance at the 98% (99%) confidence level based on the test described in section 2f. All time-series were detrended by removing the ensemble mean.

(a) Lag-corr. NW NA SST-AMOC

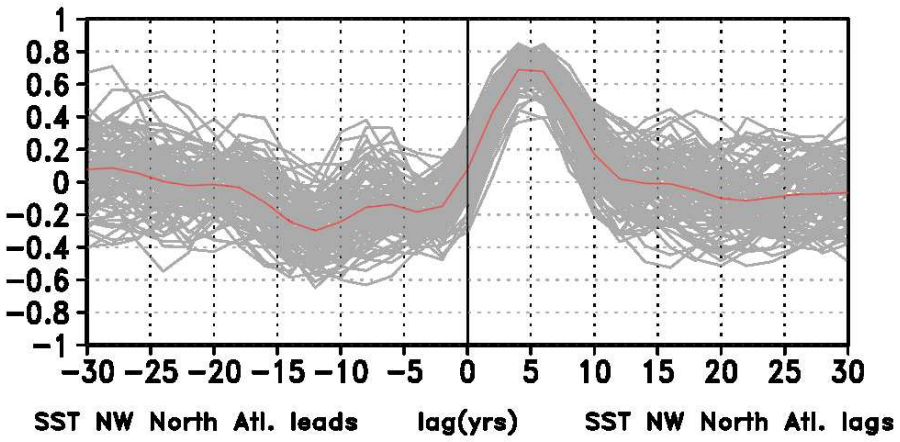

Figure S.9: (a) lag-correlation of the North-West North Atlantic SST (as previously defined) with the AMOC at 45°N in the hisorical ensemble. Red is the correlation for the entire ensemble, grey the correlations for individual ensemble members. All timeseries were demeaned and a 10-year lowpass-filter was applied.

(a) historical (b) +1 %CO_2/year

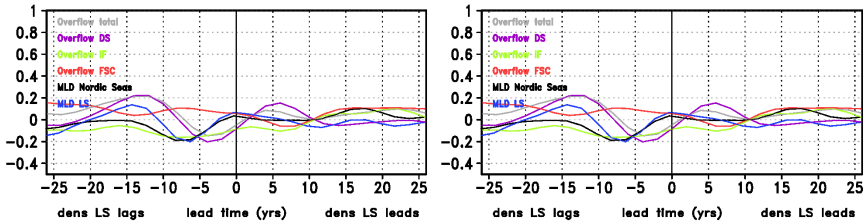

Figure S.10: Lag-correlation of the potential density (w.r.t. 2000m) averaged for the deep ocean in the Labrador Sea convection region (60-40°W, 50-60°N, 1500-3000m depth) with different indices related to the deep water formation in (a) the historical ensemble and (b) the ensemble with an incremental CO_2 increase by +1%/year. The colours indicate correlation with the volume transport of total overflow (grey), the Denmark Strait overflow (purple), the Iceland Faroer ridge overflow (greenyellow), the Faroer Scotland ridge overflow (red), and mixed layer depth in the Nordic Seas (black) and the Labrador Sea (blue). All indices were detrended by removing the ensemble mean of each quantity and 10-year low-pass-filtered.

(a) historical (b) +1%CO2/year (year 100-149

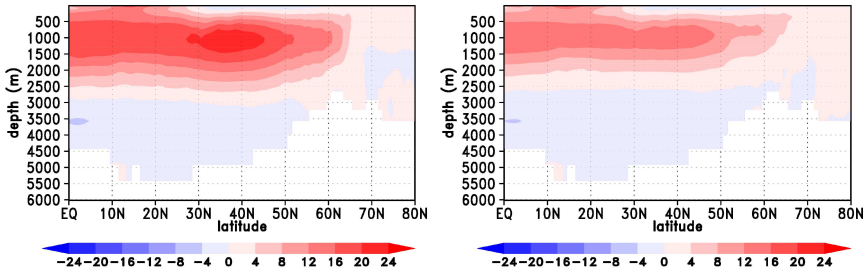

Figure S.11: Atlantic meridional overturning circulation (in Sv.) time averaged for (a) the historical ensemble and (b) the years 100-149 of the ensemble with an incremental CO_2 of 1%/year

(a) Iceland Faroer ridge density (b) Faroer Scotland ridge density

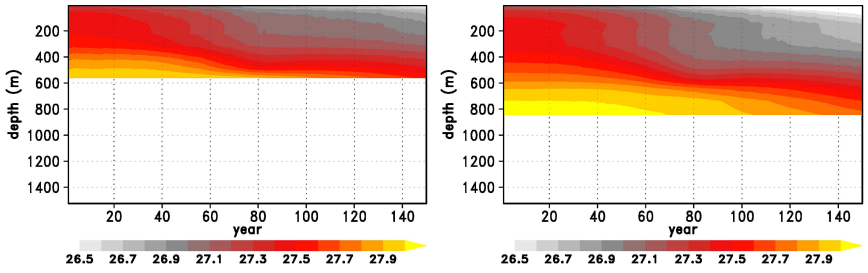

Figure S.12: Hovmoeller plot of the ocean density in the ensemble with an incremental CO_2 of 1%/year along (a) the Iceland Faroer ridge section an (b) the Faroer Scotland section. Each depth was averaged separately along the section, the timeseries are undetrended and unfiltered.

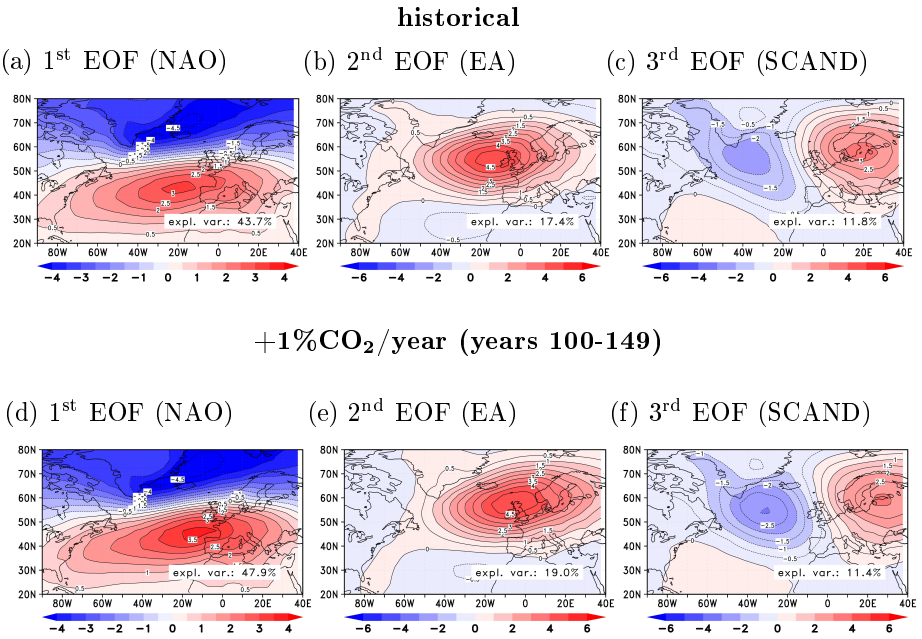

Figure S.13: Winter-time large-scale circulation variability patterns. Leading three EOF modes of December to March annual mean sea level pressure (in hPa) in the domain 90°W to 40 °E/20°N to 80 °N for the historical ensemble (top) and the years 100-149 of the ensemble with an incremental CO_2 of 1%/year (bottom).

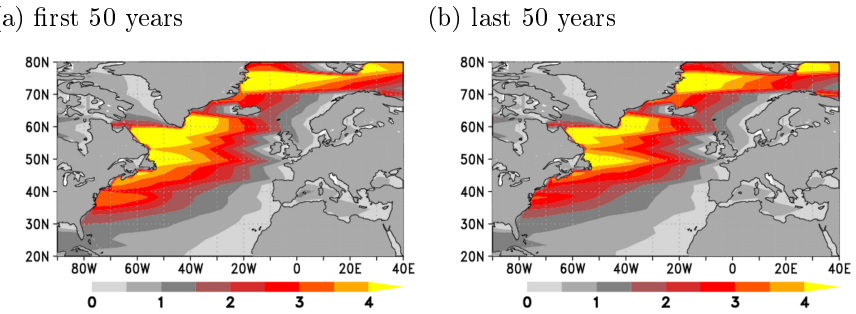

Figure S.14: Ensemble spread of the 10-year lowpass-filtered Sverdrup transport in the first (a) and the last (b) 50 years of the ensemble with an incremental CO_2 increase by +1%/year.